Effects of crystallization on the heme–carbon monoxide moiety of bovine heart cytochrome c oxidase carbonyl

Motonari Tsubaki, Kyoko Shinzawa, and Shinya Yoshikawa
Department of Life Science, Faculty of Science, Himeji Institute of Technology, Hyogo 678-12, Japan

ABSTRACT Cytochrome c oxidase isolated from bovine heart was crystallized in the fully reduced carbon monoxide (CO)-bound form. To evaluate the structure of the O_2 reaction site in crystals and in solution, the bound C–O stretch infrared band in protein crystals was compared with the band for protein solution. In solution, the C–O stretch band could be deconvoluted into two extremely narrow bands, one at 1963.6 cm^{-1} with $\Delta\nu_{1/2}$ = 3.4 cm^{-1} of 60% Gaussian/40% Lorentzian character represented 86% of the total band area and the other at 1960.3 cm^{-1} with $\Delta\nu_{1/2}$ = 3.0 cm^{-1} of 47% Gaussian/53% Lorentzian character represented 14% of the total band area. The crystals exhibited two deconvoluted C–O infrared bands having very similar band parameters with those in solution. These findings support the presence of two structurally similar conformers in both crystals and solution. Thus crystallization of this enzyme does not affect the structure at the CO-binding site to as great an extent as has been noted for myoglobin and hemoglobin carbonyls, indicating that the active (CO- or O_2-binding) site of cytochrome c oxidase must be conformationally very stable and highly ordered compared to other hemoproteins such as hemoglobin.

INTRODUCTION

Infrared spectroscopy has provided valuable information concerning the binding of ligands to various hemoproteins, including hemoglobin, myoglobin, and cytochrome *c* oxidase (CcO)[3] (1–5). Carbon monoxide (CO) is a very sensitive infrared active probe for the dioxygen-binding site because CO binds competitively and, usually, more tightly to the same site, the ferrous heme iron, and the heme-bound C–O moiety has a strong dipole moment. Configurations of the heme-CO moiety of hemoprotein–CO complexes in solutions and crystals have been evaluated by infrared spectroscopy. It is found that the discrete, interconvertible conformers of similar tertiary (or quaternary) structures, except for the vicinity of the active site that are expressed as the multiple C–O stretching modes, are present in both crystals and solutions for many hemoprotein-CO complexes (6, 7) and such interconversions can be induced upon crystallization due to the crystal lattice force and the different hydration levels. In sperm whale myoglobin (Mb), multiple C-O stretching modes were observed for the heme-bound ligand near 1933, 1944, and 1967 cm^{-1}, corresponding to three different heme–carbonyl conformers. Considerable variations in the relative proportions of the three conformers can be induced upon crystallization of Mb–CO or by incorporation of small fractions of met Mb or deoxy Mb into Mb–CO crystals (8). On the other hand, carbonyl infrared spectra of HbA–CO and Hb Zurich–CO in crystals were shown to be different from solution spectra though similar conformers are present in both crystals and solution (1). Crystallization of HbA–CO slightly shifted the ν_{C-O} and increased the width of a major band and intensified a minor band. The major band (1951.2 cm^{-1}) for HbA–CO in solution could be deconvoluted satisfactorily with only one theoretical curve, whereas in crystals at least two curves (1949.9 cm^{-1} for α subunit, and 1954.6 cm^{-1} for β subunit) were required for adequate deconvolution. Therefore the subunit difference in the IR absorbance spectrum (and in the tertiary structure around the heme) seems greater in the crystals. Thus the C–O stretch infrared band can be uniquely useful for the evaluation of crystal and solution protein structures at the ligand-binding sites.

Cytochrome *c* oxidase (CcO) is a complex protein spanning the inner mitochondrial membrane, which catalyzes the reaction:

$$O_2 + 4 \text{ cytochrome } c^{2+} + 4H^+ \rightarrow 2H_2O + 4 \text{ cytochrome } c^{3+}$$

This reaction is coupled to the generation of a proton gradient across the mitochondrial inner membrane by an unknown mechanism residing in this enzyme, and this proton gradient is the ultimate energy source for the phosphorylation of ADP. The enzyme isolated from bovine heart muscle is composed of up to 13 subunits, two hemes A (hemes *a* and a_3), two coppers as prosthetic groups along with a zinc and a magnesium, and possibly an additional copper of unknown function (9). The importance of the two hemes A and the two copper atoms in the electron transfer reaction from cytochrome *c* to dioxygen is well recognized. But the details of the structure at the dioxygen reduction site and the mechanism of the chemical steps by which dioxygen is reduced to two water molecules within this site remain to be explained.

Yoshikawa et al. (10, 11) have recently succeeded in the crystallization of CcO in the resting (oxidized) state from solutions of the enzyme from bovine heart. A crystal in hexagonal bipyramids with its space group of $P6_2$ or $P6_4$ gave x-ray diffractions as high as 7.0 Å resolution. We have successfully crystallized CcO in the fully reduced CO-bound form (CcO–CO) by a similar crystalli-

Address correspondence to Dr. Motonari Tsubaki, Department of Life Science, Faculty of Science, Himeji Institute of Technology, Kanaji 1479-1, Kamigoori-cho, Akou-gun, Hyogo 678-12, Japan.

0006-3495/92/12/1564/08 $2.00

zation procedure (Shinzawa, K., et al., unpublished results) and, in the present study, the configuration of the heme-carbonyl moiety in CcO–CO in the crystal state was evaluated by the infrared spectroscopic methods and compared with that of the solution state.

MATERIALS AND METHODS

Protein isolation. The enzyme was isolated from bovine heart muscle using Brij-35 (high purity grade; Pierce Chemical Co., Rockford, IL) as a detergent, according to the method of (10). After dialysis against 10 mM sodium phosphate buffer (pH 7.4) at 4°C, the final product in the oxidized (resting) state is freely soluble in the neutral buffer without any added detergent. The purified CcO was concentrated in 10 mM sodium phosphate buffer (pH 7.4) with a stirred ultrafiltration cell apparatus (Amicon model 80, W. R. Grace & Co., Beverly, MA) using a PTTK04310 membrane (pore size: 30,000 NMWL; Millipore Corp., Bedford, MA). The solution became turbid as a result of the formation of small crystals as the heme A concentration approached 1.5 mM. The crystals were collected by centrifugation. The preparation at this stage was used as the starting material for the crystallization of the fully reduced CO-bound form. For the determination of enzyme concentration, an extinction coefficient of $\delta_{605\text{-}630}$ = 23.3 mM^{-1} cm^{-1} for the fully reduced form in terms of heme A was used (Ueda, H., et al., unpublished observation).

Crystallization of CcO in fully reduced CO-bound state. The mechanism of the crystal growth during the concentration by ultrafiltration is due to the increase of the Brij-35 concentration in the sample solution, since micelles of Brij-35 cannot penetrate the ultrafiltration membrane. Thus Brij-35 works as a detergent at a lower concentration (close to CMC), but acts as a precipitant at a much higher concentration. This behavior as the precipitant is probably due to the long poly (oxyethylene) group of Brij-35. At a concentration much higher than CMC, a major part of Brij-35 forms micelles with the hydrophobic dodecyl ether moiety inside. Such micelles behave like poly (ethylene glycol) (PEG), a widely-used precipitant for the crystallization of proteins including CcO (Shinzawa, K., et al., unpublished observations); i.e., the poly (oxyethylene) moiety of Brij-35 competes with the hydrophilic moiety of CcO for water molecules in the solution. At a much higher concentration, the poly (oxyethylene) moiety even binds to the polar residues of CcO through hydrogen bonding, resulting in a decrease of the interaction between CcO and water molecules. This leads to the lowered solubility of CcO. The details of the crystallization procedure of CcO in the fully reduced CO-bound state will be reported elsewhere (Shinzawa, K., et al., unpublished observations). In essence, solid Brij-35 was added to the solution of CcO (~600 μM) in the oxidized state dissolved in 5 mM sodium phosphate buffer (pH 7.4) to bring the solution close to the critical point for the crystallization to occur. The solution was then treated with 5 mM sodium ascorbate under pure CO atmosphere to make the fully reduced CO-bound form. This solution was then introduced anaerobically into small test tubes containing varying amounts of solid Brij-35 to cause the crystallization. The small tubes were then sealed with silicone rubber septa and stored at 4°C under CO-atmosphere. Typically 1 to 2 weeks were needed to obtain small tetragonal crystals with an unknown space group (Fig. 1). The crystallization in the fully reduced CO-bound form was assessed by observing visible absorbance spectra of the crystals with a Hitachi 557 spectrophotometer (Fig. 2).

FT-IR Measurements. Manipulation of the crystals was carried out in a glove box saturated with pure nitrogen gas at room temperature. Small crystal fragments collected by centrifugation under the atmosphere of CO were deposited uniformly over the optical surface of the CaF_2 window of an IR cell. Excess solvent was further removed by blotting with strips of filter paper before assembling of the cell. A silicone gasket 50 μm thick was used for the assembling the IR cell. After the spectral measurements, the path length was determined from the interference pattern generated by the empty IR cell. For the solution state, the fully oxidized enzyme was deoxygenated by flowing pure nitrogen gas over the sample. The deoxygenated solution was then reduced with slight excess of sodium dithionite and pure CO gas was introduced. The resulting CcO–CO complex was then introduced into a preassembled IR cell using a disposable syringe. Formation of the carbonyl complex was confirmed by visible and infrared spectroscopies. The infrared spectra were recorded with a Perkin-Elmer model 1850 Fourier-transform infrared spectrophotometer (Perkin-Elmer Corp., Norwalk, CT) interfaced to a Perkin-Elmer 7700 computer and this system was under the control of CDS-3 application software (CDS Instruments, Oxford, PA) for data acquisition and manipulation. The infrared spectrophotometer was operated in a double beam mode. The reference IR cell contained the CcO solution in the oxidized state at the same concentration. The temperature of the IR cells was maintained at 10°C by circulating water through cell holders from a temperature-controlled water bath. Nominal spectral resolutions at 2.0, 1.0, 0.5, and 0.2 cm^{-1} were used to record the infrared spectra.

Analysis of infrared data. Infrared spectra with high signal-to-noise ratios were obtained by using high enzyme concentrations (~2 mM) combined with the spectral accumulations via Fourier-transformation of the time-based interferograms into frequency-related infrared spectral data. Typically, 200–400 cycles of spectral accumulations were required to obtain the spectra of good quality. Data points were collected every 0.03 or 0.1 cm^{-1}. Slope correction, if necessary, was made by subtracting the automatically (or manually) generated parabolic curve from the spectra in a wide spectral range (100 cm^{-1}). This subtraction technique did not affect the results obtained by the spectral deconvolution analyses, as described below, at least for very sharp bands like the C–O stretching band of CcO–CO (half bandwidths being less than 4 cm^{-1}). There was no additional averaging nor smoothing of the data. The C–O infrared band was analyzed by the spectral deconvolution using "fitg" program that contains the QUANT-3 program supplied from Perkin-Elmer Corp., in which peak frequencies (in cm^{-1}), half band widths (in cm^{-1}) and spectral shape (an arbitrary linear combination of Gaussian and Lorentzian functions) of the component bands (maximum; 11 bands) were specified manually for the calculation. The "fitg" program gives the best fitted contributions of each component band by a least-squares curve-fitting approach, which can use information from the entire spectrum rather than from a few selected frequencies. This program also can locate the baseline automatically by incorporating a sloping (or curved, if desired) baseline as an additional component in the fitting procedure. The closeness of the fitted bands to the actual spectrum can be judged by the flatness of the residual, i.e., the difference spectrum, obtained by subtracting the sum of the theoretical curves from the observed spectrum.

The integrated absorption intensities were calculated with the Perkin-Elmer model 7700 computer using a built-in program in the CDS-3 application software.

RESULTS

C–O infrared band of CcO–CO in solution state. We obtained the C–O band spectra of CcO–CO in solution state with different nominal spectral resolutions (2.0, 1.0, 0.5, and 0.2 cm^{-1}). The spectra with the resolution at 0.2 cm^{-1} had considerably lower signal-to-noise ratios, and were, therefore, not used for the analyses in the present study. The effect of the spectral resolution on the band width is summarized in Table 1. Obviously the spectral resolution at 2.0 cm^{-1} is not adequate for accurate spectral analysis of very narrow bands like the C–O stretching band of CcO–CO. Therefore, in the present study the analyses were conducted for the spectra ob-

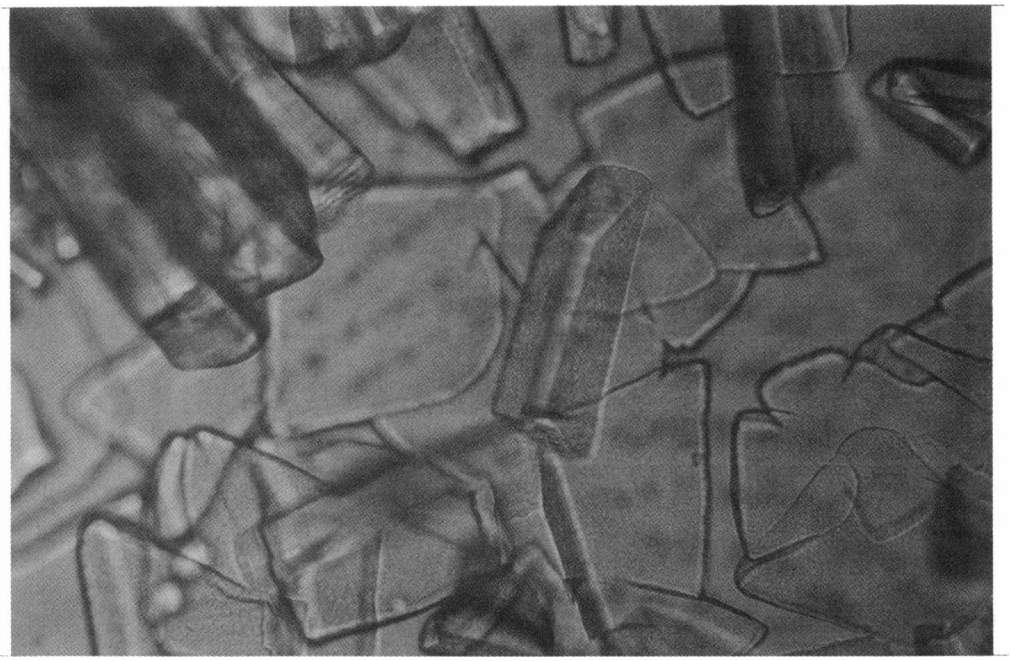

FIGURE 1 Microscopic photograph of tetragonal crystals of CcO–CO. The actual size of the photograph corresponds to about 0.65 × 0.80 mm (×150).

tained at 0.5 cm^{-1} resolution. A typical C–O band spectrum with the resolution at 0.5 cm^{-1} is shown in Fig. 3 (*top*). The observed C–O stretching band (band peak 1963.5 cm^{-1}; half bandwidth 3.7 cm^{-1}) is unusually narrow for a hemoprotein–carbonyl complex and is definitely asymmetric, suggesting the presence of more than one component. The present observation is in accordance with previous ones (12–14).

We tried first to deconvolute the C–O stretching band of CcO–CO with two Gaussian curves as suggested by Yoshikawa and Caughey (12) and then by Fiamingo, et al. (13). But a band constructed from only two Gaussian curves deviated from the observed spectrum considerably at the higher frequency side, and slightly at the lower frequency side, of the major absorbance band (Fig. 4, *top*). Introduction of a minor band around 1966.5 cm^{-1} was still inadequate (Fig. 4, *middle*), leaving reproducible deviations at both high and low frequency sides of the major absorbance. Thus 2 additional minor bands were necessary to obtain adequate fit under the restriction noted above (Fig. 4, *bottom*). This conclusion is essentially consistent with that of Einarsdóttir, et al. (14), although they found an adequate fit by the introduction of two, instead of three, minor bands on both sides of the major absorbance peak. This discrepancy is probably due to the much higher spectral resolution (0.5 cm^{-1}) obtained in this study compared to that (1.8 cm^{-1}) reported by Einarsdóttir, et al. (14). However, there is no compelling reason to use pure Gaussian curves in the deconvolution analysis (see Discussion). In the present study, we tried to deconvolute the C–O bands with a minimum number of symmetric curves

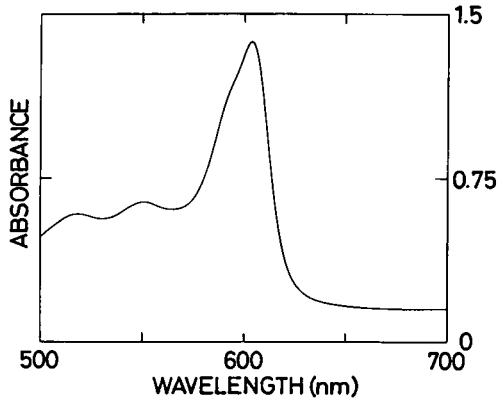

FIGURE 2 Visible absorbance spectrum of CcO–CO in tetragonal crystal state. CcO–CO crystals were sandwiched anaerobically between a hole slide glass and a slide glass and the visible absorbance spectrum was recorded with a Hitachi 557 spectrophotometer at room temperature.

TABLE 1 Effect of the spectral resolution on the observed C–O band parameters of cytochrome c oxidase–CO (CcO–CO) in solution and in crystals; the parameters are expressed as mean ± SD

Nominal resolution	Solution		Crystals	
	peak	$\Delta\nu_{1/2}$	peak	$\Delta\nu_{1/2}$
cm^{-1}	*cm^{-1}*	*cm^{-1}*	*cm^{-1}*	*cm^{-1}*
2.0	1963.6 ± 0.1	4.3 ± 0.1	1963.6 ± 0.1	4.6 ± 0.1
1.0	1963.5 ± 0.1	3.8 ± 0.1	1963.6 ± 0.1	4.4 ± 0.2
0.5	1963.5 ± 0.1	3.7 ± 0.1	1963.7 ± 0.1	4.2 ± 0.1

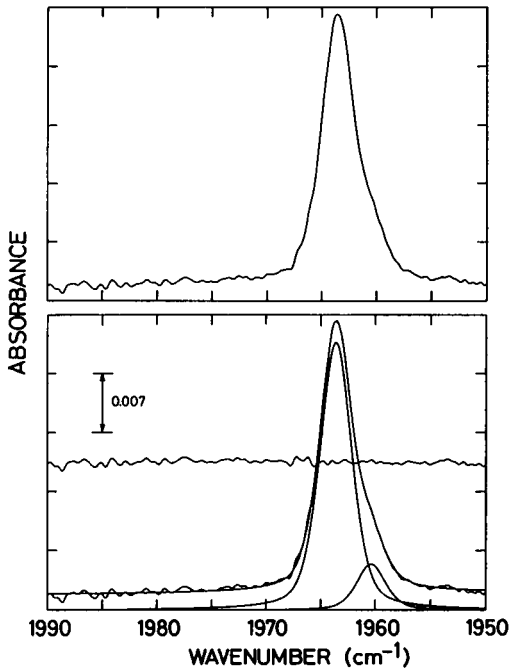

FIGURE 3 Heme-carbonyl infrared spectrum of CcO–CO in solution in 50 mM Tris-HCl buffer at pH 7.4 and 10°C and its deconvolution with theoretical curves defined by a linear combination of Gaussian and Lorentzian functions. (*Top*) The C–O infrared spectrum, slope-uncorrected. (*Bottom*) The same curve as in the top panel, deconvoluted two symmetric curves with the band parameters in solution state listed for bands A and B in Table 2, sum of the two symmetric curves, and residual spectrum (the difference between the observed spectrum and the sum of two symmetric curves). Other conditions were stated in Materials and Methods.

defined between the limits of pure Gaussian to Lorentzian functions, instead of pure Gaussian curves (see Discussion). For all the spectra obtained with spectral resolution at 0.5 cm^{-1}, adequate fits were obtained with only two symmetric bands, the major band being at 55 ~ 65% Gaussian nature. A typical result after the deconvolution analysis is shown in Fig. 3 (*bottom*). Statistics of the deconvoluted band parameters based on the latter method are summarized in Table 1.

The deconvoluted bands A and B correspond apparently to the deconvoluted bands CII (ν_{C-O} = 1959.6 cm^{-1}, $\Delta\nu_{1/2}$ = 4.0 cm^{-1}) and CIII (ν_{C-O} = 1963.4 cm^{-1}, $\Delta\nu_{1/2}$ = 4.2 cm^{-1}), respectively, reported by Einarsdóttir, et al. (14). If the contribution from the additional two minor bands (bands CI and CIV) is neglected, the band CIII contributes about 85% of the total area, which is very close to our present result (Table 1).

C–O infrared band of CcO–CO in crystals. The infrared C–O stretching band spectrum of CcO–CO in crystals with the spectral resolution at 0.5 cm^{-1} is shown in Fig. 5 (*top*) and is very similar to the spectrum in solution (Fig. 3). The crystallization caused a slight upward shift (by 0.2 cm^{-1}) of the band peak frequency to 1963.7 cm^{-1}. The half bandwidth also showed a slight increase (by 0.5 cm^{-1}) to 4.2 cm^{-1}. In addition, the shoulder around 1960 cm^{-1} was more pronounced than in the solution state. The C–O band spectra of CcO–CO crystals were analyzed by the same strategy employed for the solution state, first with pure Gaussian curves, then with curves defined by a linear combination of Gaussian and Lorentzian functions. Very similar results with those for CcO–CO in solution state were obtained (Fig. 5 and 6); for the deconvolution with pure Gaussian curves 5 bands were required (Fig. 6), whereas for the deconvolution with curves defined by a linear combination of Gaussian and Lorentzian functions adequate fits were obtained with only two symmetric bands (Fig. 5, *bottom*). Deconvoluted band parameters based on the latter method are also summarized in Table 1 and compared with those of CcO–CO in the solution state. All the band parameters for major (A) and minor (B) bands in crystals were very similar to those in solution. The relative band areas were almost identical and the ν_{C-O} values dif-

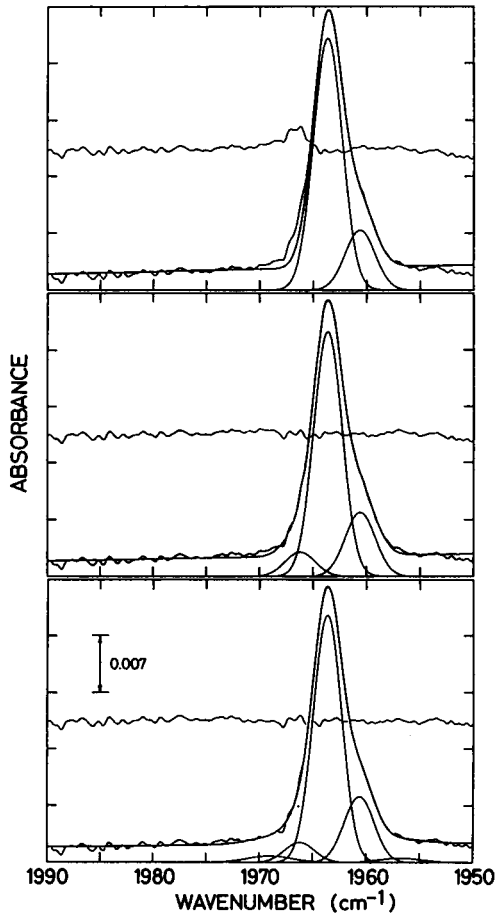

FIGURE 4 Deconvolution of the heme-carbonyl infrared spectrum of CcO–CO in solution with pure Gaussian curves. (*Top*) Deconvolution with two Gaussian curves; (*middle*) deconvolution with three Gaussian curves; bottom panel, deconvolution with five Gaussian curves. In each panel, the observed spectrum, deconvoluted theoretical curves, sum of the theoretical curves, and the difference spectrum (observed spectrum minus the sum of the deconvoluted curves) are shown.

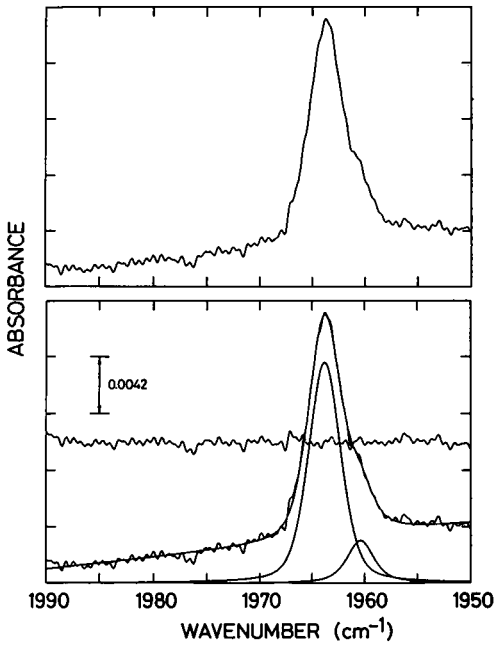

FIGURE 5 Heme-carbonyl infrared spectra of CcO–CO in crystals at 10°C. Top panel, the C–O infrared spectrum in crystal state slope-uncorrected. Bottom panel, the same curve in the top panel, two symmetric curves with the band parameters in crystals listed for bands A and B in Table 2, sum of the two symmetric curves, and residual spectrum (the difference between the observed spectrum and the sum of two symmetric curves). Other conditions are stated in Materials and Methods.

fered by 0.2 cm^{-1} for band A, and by less than 0.1 cm^{-1} for band B. The half bandwidth for band A also showed a slight increase by 0.3 cm^{-1} upon crystallization, but there was no change in band B.

Integrated absorptivity of the C–O band. The integrated absorptivity of the C–O stretch band is one of the most important characteristics of the infrared absorption band. Accuracy of the visible absorption coefficient value is apparently crucial for the determination of the integrated absorptivity. We have used a visible absorption extinction coefficient of $\mathcal{E}_{605-630} = 23.3\ mM^{-1}\ cm^{-1}$ for the fully-reduced form for the determination of the heme A concentration of CcO. This value was determined by careful and repeated examinations of metal contents in the crystalline CcO samples by atomic absorption spectrometry (Ueda, H., et al., unpublished observations). When this coefficient value was used for the calculation, the integrated C–O band absorptivity for CcO–CO was found to be 37.33 $mM^{-1}\ cm^{-2}$, very close to the corresponding value for HbA–CO, which was 35.77 $mM^{-1}\ cm^{-2}$ based on the visible absorption extinction coefficient value of $\mathcal{E}_{568.5} = 14.95\ mM^{-1}\ cm^{-1}$ in the CO form (15). Thus there is no anomaly concerning the integrated absorptivity of the C–O stretching band of CcO–CO compared to that of HbA–CO.

DISCUSSION

Two heme-carbonyl conformers in CcO–CO. It is widely accepted that ideally the true shape of a single absorption band of a liquid may be represented by a Lorentz curve (16). Band broadening can occur when a complex polyatomic molecule exists in different conformational forms in solution. If the vibrational frequencies associated with the various forms differ sufficiently, separate bands will be resolved for each form. However, if the conformational isomerism is remote from the atoms primarily involved for the vibrational frequency, the perturbation effect on the frequency will be very small, in which case it will act to broaden the band with a tendency to have Gaussian form (17). Thus for the absorption bands of the polyatomic molecules in liquid phase, both Lorentzian and Gaussian forms of broadening may be operating together, so that the resultant profile of the absorption band will be an intermediate between these two extremes (17). This is our rationale for using a linear combination of Gaussian and Lorentzian functions rather than a pure Gaussian function in the present

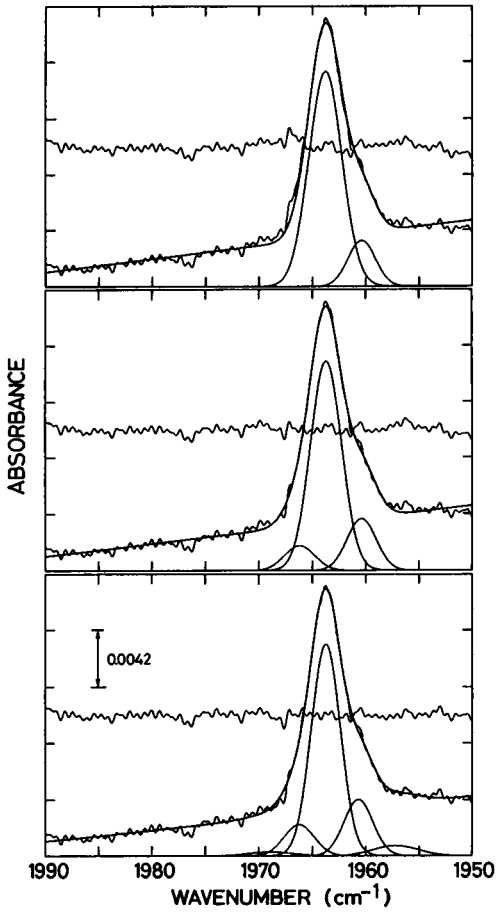

FIGURE 6 Deconvolution of the heme-carbonyl infrared spectrum of CcO–CO in crystals with pure Gaussian curves. Other conditions are the same as in Fig. 4.

TABLE 2 **Spectral band parameters of the deconvoluted infrared spectra of CcO–CO in solution and in crystals; the parameters are expressed as mean ± SD**

	Band A				Band B			
	νC–O	$\Delta\nu_{1/2}$	%G	%Area	νC–O	$\Delta\nu_{1/2}$	%G	%Area
	cm^{-1}	cm^{-1}	%	%	cm^{-1}	cm^{-1}	%	%
Solution (n = 7)	1963.6 ± 0.0	3.4 ± 0.0	60.7 ± 2.9	86.3 ± 0.7	1960.3 ± 0.1	3.1 ± 0.1	46.9 ± 7.1	13.7 ± 0.7
Crystals (n = 6)	1963.8 ± 0.1	3.7 ± 0.1	63.3 ± 3.0	85.8 ± 1.6	1960.4 ± 0.1	3.0 ± 0.1	30.3 ± 1.4	14.2 ± 1.6

study. Our strategy for the analysis was to try to deconvolute the C–O band with a minimum number of symmetric curves defined between the limits of pure Gaussian to Lorentzian function. Superficially, our deconvolution approach using a linear combination of Gaussian and Lorentzian functions may seem not much different from the conventional analysis, assuming a large number of Gaussian bands. However, there is an essential difference. Use of a linear combination of Gaussian and Lorentzian functions means the introduction of a new parameter in the analysis for determining the band shape of each conformer more precisely. On the other hand, the introduction of a new band(s) during the curve-fitting approach demands the existence of an additional conformer(s). The former approach assumes that the perturbation effect on the molecule is not large and, therefore, each existing conformer structure receives a slight modification, whereas, the latter approach postulates the strong perturbation effect on the molecule. Thus, the latter approach is energetically distinct from the former one and, therefore, should be a final choice in the analyzing procedure. Approaches similar to ours had been employed in the past by Potter et al. (1, 2)[1] and, by Shimada and Caughey (18).

It is almost certain that there were two heme-carbonyl conformers in CcO–CO solution, giving two discrete C–O stretching bands (bands A and B) (Table 2). Yoshikawa and Caughey (12) first deconvoluted the C–O stretching band of CcO–CO solution using two pure Gaussian curves. Later, Einarsdóttir et al. (14) employed a similar strategy for the spectral analysis, using four Gaussian curves, and stated that better curve-fitting was obtained by using pure Gaussian functions rather than a combination of Gaussian and Lorentzian line shapes. Our present results disagree with the latter. Only two symmetric bands, a major band with 55–65% Gaussian/35–45% Lorentzian character and a minor one with lesser Gaussian character, were sufficient to deconvolute the C–O band in our case. As a plausible explanation of the discrepancy, the spectral resolution at 1.8 cm^{-1} employed by Einarsdóttir (14) may be not enough to follow obediently the true band shape with a very narrow bandwidth (~3.7 cm^{-1}) (see Table 1).

Effects of crystallization on the C–O stretch bands. The most important finding in the present study was the existence of two very similar C–O stretching bands both in solution and in crystals (Table 2). The slight spectral changes in the band peaks (<0.2 cm^{-1}), in the half bandwidths (<0.3 cm^{-1}), or in the relative absorbance area (<1.0%) induced by the crystallization of CcO–CO (Table 2) were much less than those noted for Mb–CO and HbA–CO upon the crystallization (1, 8).

In solution, the major C–O band of HbA–CO could be deconvoluted satisfactorily with only one theoretical curve with ν_{C-O} = 1951.2 cm^{-1} and $\Delta\nu_{1/2}$ = 8.0 cm^{-1}; whereas, in crystals at least two curves (ν_{C-O} = 1949.9 cm^{-1}, $\Delta\nu_{1/2}$ = 8.0 cm^{-1} for α-subunit; ν_{C-O} = 1954.6 cm^{-1}, $\Delta\nu_{1/2}$ = 7.8 cm^{-1} for β-subunit) were necessary for an adequate deconvolution (1). Thus there were 1.3 cm^{-1} and 3.4 cm^{-1} shifts in peak position for the α-subunit and the β-subunit, respectively; although there was not much change in the half bandwidth. For Hb Zurich–CO, the corresponding shifts upon crystallization were 1.1 and 1.3 cm^{-1} for α- and β-subunits, respectively. The half bandwidths were slightly increased for both subunits (1). These peak shifts in HbA–CO and in Hb Zurich–CO upon the crystallization were far greater than the corresponding values (0.2 cm^{-1} for band A and practically nil for band B) observed for CcO–CO. For sperm whale Mb–CO, there was no quantitative data available. However, it is evident from the spectra that the relative population of each conformer changes dramatically upon crystallization (8).

Since the C–O stretch bands provide direct evidence for conformer structures and relative conformer stabilities at the dioxygen-binding site, the present observations support the presence of two structurally very similar conformers in CcO–CO, both in crystals and in solution. The dissimilar C–O infrared band behavior observed for HbA–CO, HbA Zurich–CO, Mb–CO, and

[1] We also tried the spectral analysis of the C–O band of HbA–CO, adopting the same deconvolution technique used in the present study. It was found that four symmetric bands with 55–65% Gaussian/35–45% Lorentzian character could fit the C–O absorption band satisfactorily (data not shown). Our result is consistent with reports of Potter et al. (1, 2). They analyzed the C–O stretching absorption bands of HbA–CO and Hb Zurich–CO, both in solution and in crystals, using a similar deconvolution technique to ours (1) and found that best fits were obtained with a minimum of four bands at 65% and 60% Gaussian nature for solution and crystals, respectively, of HbA–CO, and 75% and 70% for solution and crystals, respectively, of Hb Zurich–CO.

CcO–CO upon crystallization seems to reflect the different structural requirements of these proteins for carrying out their physiological functions. A flexible, dynamic protein structure at the O_2-binding site is required for these O_2-carrying proteins to permit O_2 to enter or leave without the reduction of bound O_2. For HbA such a flexible and dynamic structure is essential to perform cooperative oxygen-binding to the four heme irons by the allosteric mechanism. CcO, on the other hand, requires a ligand binding site that promotes the reduction of O_2 to water without releasing the partially reduced species (superoxide, hydrogen peroxide, and hydroxyl radicals), which are very toxic for the living cell. Thus CcO must perform as a very efficient electron sink of the electron transport system in mitochondria. For these purposes the O_2-binding site of CcO must be conformationally very stable and highly ordered, compared to other hemoproteins such as HbA. This view has been proposed previously from the very narrow C–O stretch bandwidth of CcO–CO in solution (12, 14).

Although the biochemical significance of the existence of two conformers (those give bands A and B) is not clear, it is very interesting that band B showed no spectral parameter change upon crystallization, whereas band A showed a shift in ν_{C-O} by 0.2 cm^{-1} and a widening of the band by 0.3 cm^{-1}. This result may indicate that the conformer that gives band B is more rigid than the one that gives band A. This view is consistent with the narrower bandwidth of band B than that of band A in solution state. The narrower band nature of band B than that of band A has previously been observed (12, 14), although at a much lower spectral resolution. The greater contribution of the Gaussian component in band A than in band B may have some relation to the fact that the conformer needed to give band B has a more rigid structure.

Anomalous Fe^{2+}–CO site structure in CcO–CO. The factor(s) that cause the narrowing of the C–O infrared band width of CcO–CO are of interest since this narrow C–O infrared band seems common to cytochrome *c* oxidase (19) and, therefore, must be directly, or indirectly, linked to the enzymatic functions (O_2-reduction to water and proton pumping). The very narrow C–O stretch bandwidth may be due to the extensive hydrogen bonding to the bound carbon monoxide from the distal residue(s), since such an anomalous narrowing is observed for the Fe^{2+}–CO stretching Raman band of the form II of CCP–CO in which a strong distal hydrogen bonding is expected (20, 21). From the relative location of the data point for CcO–CO in the "ν_{Fe-CO} versus ν_{C-O} plot" (3–5),[2] however, an indication that the distal hydrogen-bonding to bound C–O is not significant in the heme pocket may be inferred, based on the following reasons. First, the distal effect will increase the drift of electrons from the Fe(d_π) to the CO(π^*) orbitals and the developing charge is stabilized by the interaction with the distal hydrogen-bonding. This causes a shift to the high end along the line in the plot (22), as observed for the forms II of HRP–CO (with ν_{C-O} = 1904 cm^{-1}, ν_{Fe-CO} = 537 cm^{-1}) (23) and CCP–CO (with ν_{C-O} = 1922 cm^{-1}, ν_{Fe-CO} = 530 cm^{-1} (20). The relative location of the data point for CcO–CO in the plot seems not so significantly different from those with usual hemoprotein–CO complexes having no appreciable distal hydrogen-bonding (such as HbA–CO and Mb–CO), because the ν_{C-O} = 1963 cm^{-1} of CcO–CO is usual as a hemoprotein carbonyl. Second, if the hydrogen atom at the distal residue is exchangeable, there should be a substantial D_2O shift in the C–O stretching frequency. Indeed for HRP–CO and CCP–CO, such strong hydrogen-bonding to the bound C–O was experimentally demonstrated by the measurable D_2O shifts (2.5 cm^{-1} downshift for HRP–CO form II (24), and 2.0 cm^{-1} downshift for CCP–CO form II (25). However, in CcO–CO, an upward shift of only 0.2 cm^{-1} was observed upon the D_2O substitution (14) (Tsubaki, M., and S. Yoshikawa, unpublished observation). Thus there must be an unknown factor(s), other than hydrogen bonding to the bound carbon monoxide, causing the narrow C–O infrared bandwidth of CcO–CO. It is likely that the existence of Cu_B in close proximity to the bound C–O is responsible, at least in part, for the narrow C–O stretch bandwidth and for the other anomaly, i.e., the high value of the Fe–CO stretching mode (520 cm^{-1}) (26) compared to the usual value of the C–O stretching mode (1963.3 cm^{-1}).

In conclusion, FT–IR spectroscopy of heme-carbonyl moiety in CcO–CO revealed the presence of two structurally similar conformers, both in solution and in crystals. The crystallization of this enzyme does not affect the structures at the carbon monoxide binding site to as great an extent as has been observed for myoglobin and hemoglobin carbonyl. Therefore an x-ray crystal structure of CcO–CO will be pertinent to understanding the solution structure of this enzyme.

We thank Mr. Y. Yamashita of Himeji Institute of Technology for technical assistance during the preparation of CcO–CO crystals.

Part of this work was supported by a grant-in-aid from the Ministry of Education, Culture and Science of Japan.

Received for publication 1 April 1992 and in final form 28 July 1992.

[2] For many imidazole-Fe^{2+}–CO complexes a good inverse correlation was found between the frequencies of ν_{Fe-CO} and ν_{C-O}, i.e., the data points follow a straight line (3, 4) given by

$$\nu_{Fe-CO}(cm^{-1}) = 1935 - 0.73\nu_{C-O}(cm^{-1})$$

(reference 5).

REFERENCES

1. Potter, W. T., R. A. Houtchens, and W. S. Caughey. 1985. Crystallization-induced changes in protein structure observed by infra-

red spectroscopy of carbon monoxide liganded to human hemoglobin A and Zurich. *J. Am. Chem. Soc.* 107:3350–3352.

2. Potter, W. T., J. H. Hazzard, M. G. Choc, M. P. Tucker, and W. S. Caughey. 1990. Infrared spectra of carbonyl hemoglobins: Characterization of dynamic heme pocket conformers. *Biochemistry.* 29:6283–6295.
3. Tsubaki, M., and Y. Ichikawa. 1985. Resonance Raman detection of a ν(Fe–CO) stretching frequency in cytochrome P-450$_{scc}$ from bovine adrenocortical mitochondria. *Biochim. Biophys. Acta.* 827:268–274.
4. Tsubaki, M., A. Hiwatashi, and Y. Ichikawa. 1986. Effects of cholesterol and adrenodoxin binding on the heme moiety of cytochrome P-450$_{scc}$: A resonance Raman study. *Biochemistry.* 25:3563–3569.
5. Li, X.-Y., and T. G. Spiro. 1988. Is bound CO linear or bent in heme proteins? Evidence from resonance Raman and infrared spectroscopic data. *J. Am. Chem. Soc.* 110:6024–6033.
6. Choc, M. G., and W. S. Caughey. 1981. Evidence from infrared and ^{13}C NMR spectra for discrete rapidly interconverting conformers at the carbon monoxide binding sites of hemoglobins A and Zurich. *J. Biol. Chem.* 256:1831–1838.
7. Caughey, W. S., H. Shimada, M. G. Choc, and M. P. Tucker. 1981. Dynamic protein structures: Infrared evidence for four discrete rapidly interconverting conformers at the carbon monoxide binding site of bovine heart myoglobin. *Proc. Natl. Acad. Sci. USA.* 78:2903–2907.
8. Makinen, M. W., R. A. Houtchens, and W. S. Caughey. 1979. Structure of carboxymyoglobin in crystals and in solution. *Proc. Natl. Acad. Sci. USA.* 76:6042–6046.
9. Palmer, G. 1987. Cytochrome oxidase: a perspective. *Pure Appl. Chem.* 59:749–758.
10. Yoshikawa, S., T. Tera, Y. Takahashi, T. Tsukihara, and W. S. Caughey. 1988. Crystalline cytochrome *c* oxidase of bovine heart mitochondrial membrane: Composition and x-ray diffraction studies. *Proc. Natl. Acad. Sci. USA.* 85:1354–1358.
11. Yoshikawa, S., K. Shinzawa, T. Tsukihara, T. Abe, and W. S. Caughey. 1991. Crystallization of beef heart cytochrome *c* oxidase. *J. Crystal Growth.* 110:247–251.
12. Yoshikawa, S., and W. S. Caughey. 1982. Heart cytochrome *c* oxidase. An infrared study of effects of oxidation state on carbon monoxide binding. *J. Biol. Chem.* 257:412–420.
13. Fiamingo, F. G., R. A. Altschuld, P. P. Moh, and J. O. Alben. 1982. Dynamic interactions of CO with a_3Fe and Cu_B in cytochrome *c* oxidase in beef heart mitochondria studied by Fourier transform infrared spectroscopy at low temperature. *J. Biol. Chem.* 257:1639–1650.
14. Einarsdóttir, O., M. G. Choc, S. Weldon, and W. S. Caughey. 1988. The site and mechanism of dioxygen reduction in bovine heart cytochrome *c* oxidase. *J. Biol. Chem.* 263:13641–13654.
15. Banerjee, R., Y. Alpert, F. Leterrier, and R. J. P. Williams. 1969. Visible absorption and electron spin resonance spectra of the isolated chains of human hemoglobin. Discussion of chain-mediated heme–heme interaction. *Biochemistry.* 8:2862–2867.
16. Ramsay, D. A. 1952. Intensities and shapes of infrared absorption bands of substances in the liquid phase. *J. Am. Chem. Soc.* 74:72–80.
17. Seshardi, K. S., and R. N. Jones. 1963. The shapes and intensities of infrared absorption bands—A review. *Spectrochim. Acta.* 19:1013–1085.
18. Shimada, H., and W. S. Caughey. 1982. Dynamic protein structures. Effects of pH on conformer stabilities at the ligand-binding site of bovine heart myoglobin carbonyl. *J. Biol. Chem.* 257:11893–11900.
19. Young, L. J., O. Einarsdóttir, C. R. Vossbrink, and W. S. Caughey. 1984. Infrared spectra of carbon monoxide bound to mitochondria from diverse species and tissues reveal structurally similar cytochrome *c* oxidase dioxygen reaction sites. *Biochem. Biophys. Res. Commun.* 123:247–253.
20. Smulevich, G., R. Evangelista-Kirkup, A. English, and T. G. Spiro. 1986. Raman and infrared spectra of cytochrome *c* peroxidase–carbon monoxide adducts in alternative conformation states. *Biochemistry.* 25:4426–4430.
21. Smulevich, G., J. M. Mauro, L. A. Fishel, A. M. English, J. Kraut, and T. G. Spiro. 1988. Cytochrome *c* peroxidase mutant active site structures probed by resonance Raman and infrared signatures of the CO adducts. *Biochemistry.* 27:5486–5492.
22. Spiro, T. G., G. Smulevich, and C. Su. 1990. Probing protein structure and dynamics with resonance Raman spectroscopy: Cytochrome *c* peroxidase and hemoglobin. *Biochemistry.* 29:4497–4508.
23. Evangelista-Kirkup, R., G. Smulevich, and T. G. Spiro. 1986. Alternative carbon monoxide binding modes for horseradish peroxidase studied by resonance Raman spectroscopy. *Biochemistry.* 25:4420–4425.
24. Smith, M. L., P.-I. Ohlsson, and K. G. Paul. 1983. Infrared spectroscopic evidence of hydrogen bonding between carbon monoxide and protein in carbonylhorseradish peroxidase C. *FEBS (Fed. Eur. Biochem. Soc.) Lett.* 163:303–305.
25. Satterlee, J. D., and J. E. Erman. 1984. Deuterium isotope effect on the heme-coordinated CO vibration band of ferrous cytochrome *c* peroxidase-CO. *J. Am. Chem. Soc.* 106:1139–1140.
26. Argade, P. V., Y. Ching, and D. L. Rousseau. 1984. Cytochrome a_3 structure in carbon monoxide-bound cytochrome oxidase. *Science (Wash. DC).* 225:329–331.